Resonant and phonon-assisted excitation energy transfer in the R_1 line of $[Cr(ox)_3]^{3-}$

Marianne E. von Arx and Andreas Hauser*

Institut für Anorganische und Physikalische Chemie, Universität Bern, Freiestrasse 3, CH-3000 Bern 9, Switzerland

Hans Riesen

Research School of Chemistry, The Australian National University, Canberra ACT 0200, Australia

René Pellaux and Silvio Decurtins

Institut für Anorganische Chemie der Universität Zürich, Winterthurerstrasse 190, CH-8057 Zürich, Switzerland

In resonant fluorescence line narrowing (FLN) experiments in the R_1 transition of the $[Cr(ox)_3]^{3-}$ chromophore in $[Ru(bpy)_3][NaAl:Cr(1\%)(ox)_3]$ and $[Rh(bpy)_3][NaCr(ox)_3]ClO_4$ multiline spectra are observed at 1.8 K, (ox=oxalate, bpy=2,2'-bipyridine). For $[Rh(bpy)_3][NaCr(ox)_3]ClO_4$ the number of lines and their relative intensities depend critically upon the excitation wavelength within the inhomogeneous distribution, and in time-resolved FLN experiments additionally upon the delay. This behavior is clear evidence for a resonant energy-transfer process. At 4.2 K the more common phonon-assisted process becomes dominant, manifesting itself as spectral diffusion. [S0163-1829(96)04746-7]

I. INTRODUCTION

Excitation energy transfer between identical chromophores in solids containing transition-metal ions has been the subject of a large number of studies.[1,2] In particular energy migration within the electronic origin of the low-energy component of the ^2E state of Cr^{3+} doped into Al_2O_3 (ruby), the so-called R_1 line, has been extensively discussed.[1] Fluorescence line narrowing (FLN) experiments at 10 K on $Al_2O_3:Cr^{3+}(0.9\%)$ performed by Selzer and co-workers[3,4] indicate that single ion to single ion energy transfer proceeds mainly via spectral diffusion and is thus a phonon-assisted process, showing a typical linear dependence of the transfer rate with temperature.[5] Somewhat later Chu *et al.*[6] and Jessop and Szabo[7] succeeded in observing slow resonant single-ion energy transfer based on electric-field experiments. The transfer times on the millisecond time scale were found to be compatible with a dipole-dipole mechanism. However, this pertains to resonant energy transfer from Cr^{3+} ions on the one sublattice to Cr^{3+} ions on the other. Duval and Monteil[8] maintain that within one sublattice resonant energy transfer is rapid based on uniaxial stress experiments. In addition to experiments on ruby, other Cr^{3+}-doped systems have been investigated,[9] but in no instance was there any clear cut evidence for a fast resonant process.

In a preliminary report[10] evidence for such a resonant process in the three-dimensional network structure $[Rh(bpy)_3][NaCr(ox)_3]ClO_4$ (ox=oxalate, bpy=2,2'-bipyridine) was presented. The compound crystallizes in the cubic space group $P2_13$,[11] with the $[Cr(ox)_3]^{3-}$ units having C_3 point symmetry. The basic spectroscopic behavior is identical to the one of the large number of octahedrally coordinated and trigonally distorted Cr^{3+} chromophores[12,13] studied to date, with a comparatively large splitting of the lowest excited ^2E state, and a small zero-field splitting of the $^4A_2$ ground state which is usually obscured by the inhomo-geneous width of the R lines. The present paper is a full account of our studies of excitation energy transfer in $[Rh(bpy)_3][NaCr(ox)_3]ClO_4$. Time-resolved FLN techniques allow for a clear distinction between the more common phonon-assisted process and the resonant process.

II. EXPERIMENT

The two compounds $[Ru(bpy)_3][NaAl:Cr(1\%)(ox)_3]$ and $[Rh(bpy)_3][NaCr(ox)_3]ClO_4$ were prepared as described in Refs. 14 and 11. Spectroscopic measurements were performed on a single crystal (1 mm edge) of the former and polycrystalline samples of the latter.

Broadband luminescence spectra were obtained by exciting with a He-Ne laser at 543 nm (Polytec PL 405 GR). For fluorescence line narrowing experiments a Ti:sapphire laser (Schwartz Electro Optics) was used, pumped by an argon-ion laser (Spectra Physics 2045-15/4S). Equipped with an étalon, the laser linewidth was ≤ 0.02 cm^{-1}. The luminescence was dispersed by a 3/4 m double monochromator (Spex 1402). A cooled photomultiplier (RCA-C31034) was used as detector, and the signal was processed by a gated photon counting system (Standford Research 400). In the FLN spectra the experimental resolution is limited by the monochromator (0.3 cm^{-1}, 15 μm slits). In the resonant FLN experiments the exciting laser beam and the resulting luminescence were both passed through the same chopper blade, but with a phase shift of 180° in order to avoid laser light reaching the photomultiplier tube.[15]

For time-resolved measurements a photoelastic modulator (Coherent 305) was used in addition to the mechanical chopper in order to produce laser pulses of $\sim 1-4$ μs. The time-resolved luminescence was recorded using the gated photon counting system at fixed delays for full spectra and a multichannel scaler (Standford Research 403) for decay curves.

Highly resolved FLN spectra were obtained using a single frequency dye laser and a scanning plane parallel Fabry-
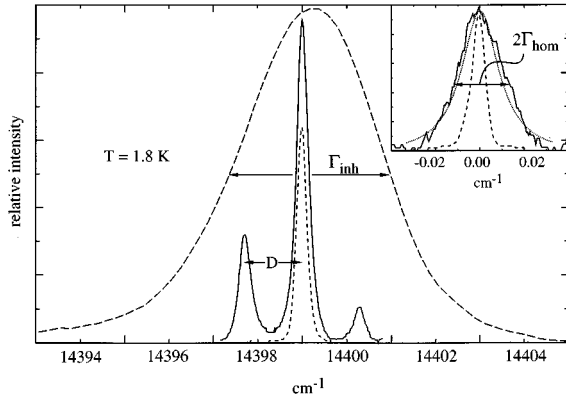
FIG. 1. Luminescence spectra in the region of the R_1 line of $[Ru(bpy)_3][NaAl:Cr(1\%)(ox)_3]$ at 1.8 K. (— — — —) Excitation into the $^4A_2 \rightarrow {}^4T_2$ transition at 543 nm, $\Gamma_{inh}=4$ cm^{-1}; (____) resonant FLN spectrum using the Fabry-Pérot interferometer at 100 GHz free spectral range, zero-field splitting of the $^4A_2$ ground state $D=1.3$ cm^{-1}; (- - - -) instrumental response. Inset: resonant line of the FLN spectrum at 3 GHz free spectral range. (____) Experimental; ($\cdot \cdot \cdot \cdot$) Lorentzian fit, $\Gamma_{hom}=0.012$ cm^{-1} (360 MHz); (– – – – –) instrumental response.

Pérot interferometer (Burleigh RC-110) described elsewhere.[10,15]

For excitation spectra the Ti:sapphire laser was scanned using an inchworm controller (Burleigh PZ 500-1) without the étalon, and the wavelength was monitored with a wavemeter (Burleigh Jr). Sample temperatures between 1.8 and 4.2 K were achieved in a pumped He bath cryostat (Oxford Instruments MD 4). Model calculations for the energy-transfer processes, in particular solving a set of coupled differential equations numerically, were performed using the ACSL (Ref. 16) subroutine package.

III. RESULTS

A. Luminescence and excitation spectra

Upon excitation at 18 416 cm^{-1} (543 nm), that is into the $^4T_2$ absorption band of the $[Cr(ox)_3]^{3-}$ chromophore in both the diluted $[Ru(bpy)_3][NaAl:Cr(1\%)(ox)_3]$ system as well as in the neat $[Rh(bpy)_3][NaCr(ox)_3]ClO_4$, sharp line luminescence assigned to the $^2E \rightarrow {}^4A_2$ transition is observed.[17,11] The splitting of the ^2E state is 13.2 cm^{-1} for the latter and 14.9 cm^{-1} for the former.

Figure 1 shows the luminescence spectrum for excitation at 543 nm of a single crystal of $[Ru(bpy)_3][NaAl:Cr(1\%)(ox)_3]$ in the region of the lower-energy electronic origin of the $^2E \rightarrow {}^4A_2$ transition (R_1 line) at 1.8 K. The line shape is close to Gaussian centered at 14 399.3 cm^{-1}, with a full width at half maximum of ~ 4 cm^{-1}. With a spectral resolution of 0.3 cm^{-1} the latter value thus corresponds to the inhomogeneous width Γ_{inh} of the transition.

Spectrum (a) in Fig. 2 shows the corresponding luminescence at 1.8 K for a microcrystalline sample of $[Rh(bpy)_3][NaCr(ox)_3]ClO_4$. In luminescence, the maximum of the R_1 line of the neat material is at 14 396.9 cm^{-1}. For the excitation spectrum, spectrum (b) in Fig. 2, the luminescence was detected nonselectively in a vibra-
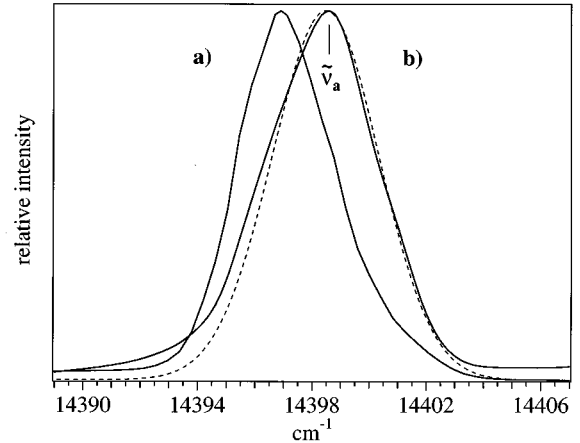
FIG. 2. (a) Luminescence spectrum of $[Rh(bpy)_3][NaCr(ox))_3]ClO_4$ in the region of the R_1 line at 1.8 K upon nonselective excitation at 543 nm. (b) Excitation spectrum at 1.8 K, monitored at 14 368 cm^{-1} (____), and best fit with Gaussian distribution for the excited state, a ground-state zero-field splitting D of 1.3 cm^{-1} and relative oscillator strengths for the two components of 2.8:1 as determined for the diluted system. The maximum is close to the high-energy component of the R_1 line, $\tilde{\nu}_a$.

tional side band at 14 368 cm^{-1} using a comparatively large bandwidth of 2 cm^{-1}. As for the luminescence, an approximately Gaussian line shape with an inhomogeneous width Γ_{inh} of 4.4 cm^{-1} is observed. This is slightly larger than the 3.8 cm^{-1} observed in luminescence, and with 14 398.6 cm^{-1} the maximum is shifted towards higher energies by 1.7 cm^{-1} with respect to the luminescence.

B. Resonant fluorescence line narrowing (FLN)

The zero-field splitting of the $^4A_2$ ground state, D, is smaller than the inhomogeneous line width Γ_{inh} and is not resolved in the above spectra. In such a case, a resonant FLN spectrum of the R_1 line of Cr^{3+} characteristically consists of three lines: the central, resonant line, and satellites at $\pm D$.[1,15,18] The relative intensities of the three lines depend upon the sample temperature, the relative transition probabilities of the two overlapping transitions, and upon the excitation wavelength within the inhomogeneous distribution. In the doped system $[Ru(bpy)_3][NaAl:Cr(1\%)(ox)_3]$ these expectations are met (see Fig. 1) and the observed splitting gives a value for D of 1.3 cm^{-1}. The ratio of the intensities of the satellites at $-D$ and $+D$ of 1:0.35 conforms to a Boltzmann distribution between the zero-field components of the $^4A_2$ ground state at 1.8 K. From the relative intensity of the satellites to the central line, a ratio for the radiative transition probabilities between the two ground-state levels and the lower-energy level of the ^2E state of 2.8:1 can be extracted. Furthermore, using a single-frequency dye laser and a Fabry-Pérot interferometer,[15] the homogeneous linewidth of the R_1 line, Γ_{hom}, is found to be ~ 0.012 cm^{-1} (360 MHz) at 1.8 K (inset Fig. 1).

The resonant FLN spectra at 1.8 K of neat $[Rh(bpy)_3][NaCr(ox)_3]ClO_4$ shown in Fig. 3 consist of
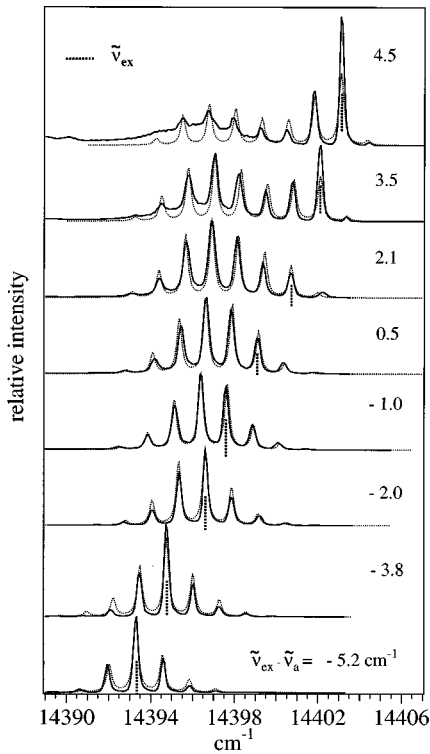
FIG. 3. (———) resonant FLN spectra of $[Rh(bpy)_3][NaCr(ox)_3]ClO_4$ at 1.8 K as a function of the laser frequency $\tilde{\nu}_{ex}$ within the inhomogeneous width of the R_1 line (· · · ·). Simulated resonant FLN spectra using the parameters relevant for the $[Cr(ox)_3]^{3-}$ chromophore as given in the text and $k'_{et} = 10^4$ s^{-1}. $\tilde{\nu}_{ex} - \tilde{\nu}_a$ is the energy difference between excitation energy and the maximum of the absorption.

FIG. 4. Temperature dependence of the resonant FLN spectrum of $[Rh(bpy)_3][NaCr(ox)_3]ClO_4$ in the region of the R_1 line between 1.8 and 4.2 K, $\tilde{\nu}_{ex} = 14\ 399.0$ cm^{-1}.

many more lines than the simple three-line spectrum. The spacing between adjacent lines is 1.3 cm^{-1} throughout the spectrum, that is, equal to D, but the number of lines observed and their relative intensities depend critically upon the excitation energy $\tilde{\nu}_{ex}$ relative to the maximum of the R_1 line in the excitation spectrum $\tilde{\nu}_a$. Only for excitation at the low-energy edge of the inhomogeneous distribution does the spectrum resemble the three-line spectrum observed for the diluted compound, for which the resonant line is always the most intense. Excitation more at the center of the distribution results in additional lines both at higher and lower energies, but with a bias towards those at lower energies. Furthermore, in contrast to the diluted compound, the resonant line is not always the most intense.

C. Temperature dependence

In Fig. 4 the steady-state FLN spectra obtained at temperatures between 1.8 and 4.2 K are presented for an excitation wavelength on the high-energy side of the excitation maximum. The multiline patterns at 1.8 and 2.4 K are very similar, with only a hint of an additional background at 2.4 K. Above 2.4 K this background grows strongly with increasing temperature. However, the intensity ratios of the sharp lines are not affected by the background, that is, they are temperature independent. At 4.2 K, the spectrum is domi-

nated by the broad background and is nearly the same as spectrum (a) in Fig. 2 resulting upon excitation into the $^4A_2 \rightarrow {}^4T_2$ transition.

D. Time dependence

Time-resolved FLN experiments were performed at 1.8, 3.0, and 4.2 K (see Fig. 5). As for the temperature-dependent steady-state spectra, the excitation was effected close to the absorption maximum and in pulses of ~ 4 μs width. The spectra were recorded at different delay times following the excitation pulse and widths from 4 μs for short delays to 50 μs for longer delays. Figure 5(a) shows the resulting spectra at 1.8 K. Shortly after the pulse (delay time $= 4$ μs, gate width $= 4$ μs) the three-line pattern with spacings of 1.3 cm^{-1}, as observed for the diluted systems, is obtained. At longer delay times multiline patterns begin to appear. The number of lines increases with increasing delay time and the maximum intensity shifts towards lower energies. The same experiments were performed at 3.0 and 4.2 K. The spectra are given in Figs. 5(b) and 5(c), respectively. At 4.2 K the spectrum recorded immediately after the pulse is a three-line spectrum identical to the one at 1.8 K. After a 50 μs delay time, a broad background appears in addition to the multiline pattern. After 200 μs this background dominates the line shape and the sharp lines are not observed anymore. This is in contrast to the spectra at 1.8 K where also for long delay times (1250 μs) no broad background can be seen. The spectra obtained at 3.0 K show virtually the same behavior as the spectra at 4.2 K, with the exception of the rise time of the broad background being longer. The relative intensities of
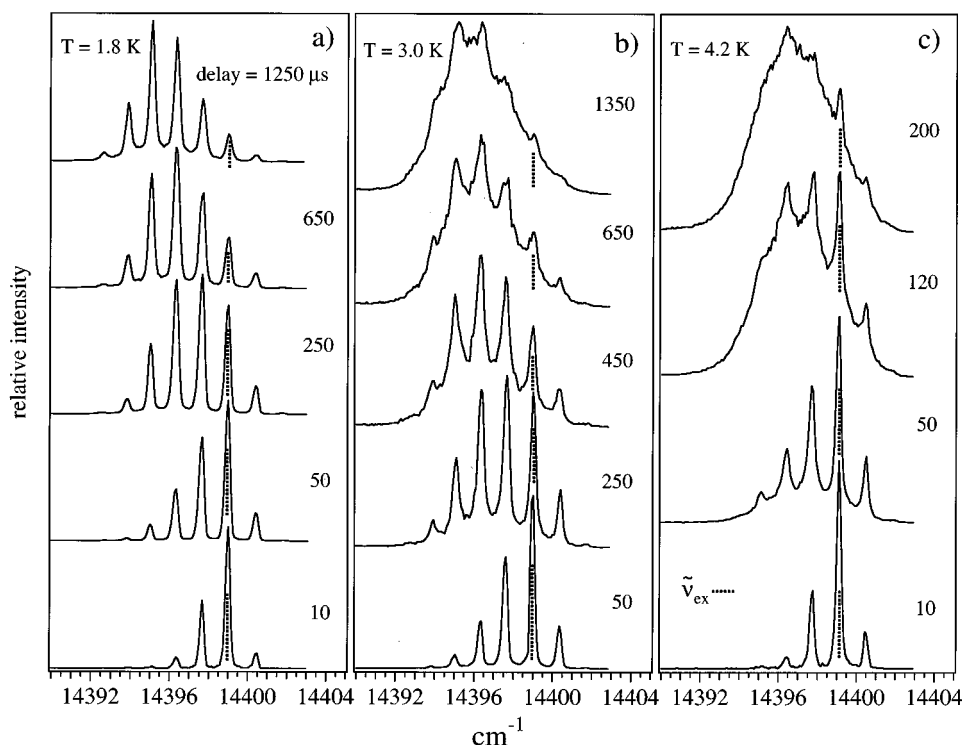
FIG. 5. Time-resolved resonant FLN spectra of $[Rh(bpy)_3][NaCr(ox)_3]ClO_4$ in the region of the R_1 line at (a) 1.8 K, (b) 3.0 K, and (c) 4.2 K. The delay times in μs are indicated in the figure, $\tilde{\nu}_{ex} = 14\ 399.0$ cm^{-1}.

the sharp lines at 1.8, 3.0, and 4.2 K of the corresponding delay times are equal within the experimental accuracy.

The sharp lines in the spectra are numbered in the following way: the resonant line at which excitation takes place is called line 0, the lines lying at higher energies $+i$ ($i=1,2\ldots$) and the ones at lower energies $-i$. Figure 6(a) shows the luminescence decay curves at 1.8 K of lines $i=+1,0,-1,\ldots,-4$ following pulsed excitation ($\sim 1\ \mu$s pulse length) at 14 399.7 cm^{-1}. The decay curve of the resonant line, $i=0$, is characterized by a fast nonexponential decay. The decay curves of the other lines show a build-up, followed by a nonexponential decay. For lines close to the excitation energy (small i), the rise time is short, for example

$\sim 100\ \mu$s for line $i=-1$. With increasing energy difference between excitation and detection (larger i) the rise time becomes longer, for instance $\sim 700\ \mu$s for line $i=-4$. At long times the decay curve of line $i=-4$ shows a single exponential behavior. The exponential fit of this last part of the curve results in a decay time of 1.3 ms, which is equal to decay times observed in diluted $[Cr(ox)_3]^{3-}$ systems. The 1.3 ms correspond to the radiative lifetime τ_r of the ^2E state and are in good agreement with the observed oscillator strength for the $^4A_2 \rightarrow {}^2E$ transition.[17] The resolution used to measure the decay curves shown in Fig. 6(a) was not high enough to avoid partial recording of neighboring lines $i \pm 1$.
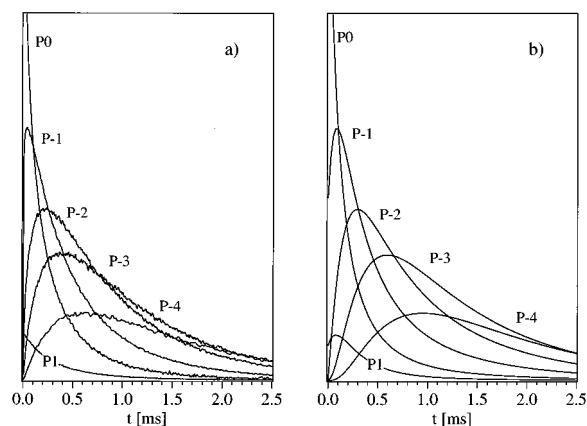
FIG. 6. Time-resolved resonant FLN experiment at 1.8 K of $[Rh(bpy)_3][NaCr(ox)_3]ClO_4$: (a) Experimental decay curves of the individual peaks as labeled in Fig. 4 of the multiline spectrum upon pulsed excitation at $\tilde{\nu}_{ex} = 14\ 399.7$ cm^{-1}. (b) Calculated decay curves using the parameters relevant for the $[Cr(ox)_3]^{3-}$ chromophore given in the text and $k'_{et} = 10^4$ s^{-1}.

IV. DISCUSSION

At liquid-helium temperatures only three levels of octahedrally coordinated Cr^{3+} have to be considered (see Fig. 7): first, the two zero-field components of the $^4A_2$ ground state (g_a and g_b) and, second, the low-energy component the ^2E state (e). With a splitting of 13 cm^{-1}, the high-energy component of the ^2E state can be neglected at temperatures below 4.2 K.

For the diluted $[Ru(bpy)_3][NaAl:Cr(1\%)(ox)_3]$ system, the expected three-line pattern is observed in the FLN spectrum (see Fig. 1), from which it is straightforward to extract values for the zero-field splitting D of the $^4A_2$ ground state, the homogeneous linewidth Γ_{hom}, and the ratio of the radiative rate constants k_a/k_b of 1.3 cm^{-1}, 0.012 cm^{-1}, and 2.8:1, respectively. For the diluted compound the total radiative decay rate constant k_r is $1/\tau_r = k_a + k_b = 770$ s^{-1}.

In concentrated systems energy transfer in the R_1 line of the ^2E state is often encountered. The redshift of the R_1 line in luminescence by 1.7 cm^{-1} with respect to the excitation as well as the slightly smaller inhomogeneous linewidth of

FIG. 7. Schematic representation of the model for resonant and phonon-assisted energy transfer in the R_1 transition of Cr^{3+}. Parameters are explained in the text.

the former (see Fig. 2) indicate that energy-transfer processes are important in neat $[Rh(bpy)_3][NaCr(ox)_3]ClO_4$. In FLN experiments energy transfer is usually observed as strongly temperature-dependent spectral diffusion[1,3,4] from the narrowed three-line spectrum into the inhomogeneous distribution, and is therefore a phonon-assisted process. This behavior is indeed observed in the FLN spectrum of $[Rh(bpy)_3][NaCr(ox)_3]ClO_4$ at 4.2 K. As the temperature is lowered to below 4.2 K this process freezes out (see Fig. 4).

The multiline FLN spectra of $[Rh(bpy)_3][NaCr(ox)_3]ClO_4$ observed at 1.8 K call for a different explanation. The model presented in the following postulates a resonant energy-transfer process in addition to the nonresonant spectral diffusion. Figure 7 depicts the basic assumptions of the model. The inhomogeneous distribution of transition energies is given by a Gaussian. With two inhomogeneously broadened and overlapping transitions, two sets of molecules are excited with a laser frequency $\widetilde{\nu}_{ex}$ within the inhomogeneous envelope: a set denoted as $i=0$, for which the transition $g_a \rightarrow e$ is resonant ($\widetilde{\nu}_{a0} = \widetilde{\nu}_{ex}$), and a set denoted $i=1$, for which the transition $g_b \rightarrow e$ is resonant ($\widetilde{\nu}_{b1} = \widetilde{\nu}_{ex}$). Resonant energy transfer is possible within each of these subsets individually, but because each subset has two possible transitions and because Γ_{inh} is larger than D, additional resonant energy-transfer processes are possible. For instance from the subset $i=0$ to the subset $i=-1$, for which the $g_a \rightarrow e$ transition is resonant with the $g_b \rightarrow e$ transition on subset $i=0$, or from subset $i=1$ to subset $i=2$, for which the $g_b \rightarrow e$ transition is resonant with the $g_a \rightarrow e$ transition on subset $i=1$. This results in a ladder spaced by D within the inhomogeneous distribution, with resonant energy-transfer processes between spectral neighbors i and $i \pm 1$.

Because the concentration of resonant $[Cr(ox)_3]^{3-}$ chromophores varies across the inhomogeneous distribution, the average distance between resonant chromophores, and therefore the probability for resonant energy transfer, varies too (Anderson localization[19,20]). Consequently, the structure of the multiline pattern depends strongly upon the excitation wavelength: For excitation far into the low-energy tail, there

are only a few resonant chromophores, and their distance from each other is so large that hardly any resonant energy transfer can occur. Thus almost a straightforward three-line pattern is observed (see Fig. 3). The most striking multiline pattern results for excitation at or near the center of the inhomogeneous distribution, where the concentration of resonant chromophores in subsets of spectral neighbors i and $i \pm 1$ is comparatively large. At a temperature of 1.8 K there is a bias for the resonant energy transfer towards the low-energy members of the resonant ladder. This is borne out by both the steady-state spectra of Fig. 3 as well as the time-resolved spectra of Fig. 5(a), where peaks at lower energies become more intense than the resonant peak. This has also consequences for excitation into the high-energy tail (see Fig. 3). Because of the again rather low concentration of resonant chromophores the resonant peak is the most intense. But a small fraction of the energy still gets transferred down the ladder, and gets into the center of the distribution.

The steady-state spectrum at 4.2 K is dominated by spectral diffusion (see Fig. 4). Nevertheless the resonant energy transfer still takes place, as is evident from the time-resolved FLN experiments, which allow a clear distinction between the two processes [see Figs. 5(a)–5(c)]. The three-line spectrum obtained immediately after the pulse (~ 10 μs delay) both at 1.8 and at 4.2 K indicates that neither resonant nor phonon-assisted energy transfer has occurred within this short time interval. With increasing delay time the number of lines due to the resonant process increases. And in accordance with the steady-state spectra the energy mainly migrates towards lower energy. At 1.8 K only multiline patterns are obtained even at long delay times. Therefore, at this temperature the resonant energy transfer and the radiative rate are orders of magnitude faster than the phonon-assisted energy transfer. Even though phonon-assisted energy transfer becomes faster at higher temperatures, the multiline pattern is superimposed on the increasing inhomogeneously broadened luminescence. This can be seen in Figs. 5(b) and 5(c) where the broad background appears at longer delays. It is obvious that the growing-in of this background is faster at 4.2 K than at 1.8 and 3.0 K, but the relative intensities of the

sharp lines at all three temperatures and given delay times are equal within the experimental accuracy. In contrast to the phonon-assisted process, the resonant process appears to be temperature independent.

On the basis of the above, the selectively excited luminescence decay curves at 1.8 K shown in Fig. 6(a) are easily interpreted. All lines except the resonant line show a build-up due to resonant energy transfer, and except for the lowest-energy line their decays are far from single exponential. With increasing energy difference between excitation and detection the rise time becomes longer, indicating that the resonant process indeed proceeds along the steps of the ladder. The nonexponential decay of the resonant line is more than an order of magnitude faster than the radiative lifetime τ_r of 1.3 ms observed in the diluted system. This proves the resonant process to be a nonradiative process.[2] For the lowest energy line ($i = -4$) single exponential behavior with a lifetime equal to the radiative lifetime is observed at long delay times, showing that on average most of the chromophores in this low-energy subset are well separated and thus decay mainly radiatively, without being deactivated by resonant energy transfer.

In principle, the line resonant with the laser frequency should have a width equal to twice the homogeneous width Γ_{hom} as indicated in Fig. 1 for the diluted compound. For each transfer step the width should increase by an additional $2\Gamma_{\text{hom}}$. This holds for resonant energy transfer within one subset as well as for transfer to neighboring subsets. With an experimental resolution of 0.3 cm^{-1} and $\Gamma_{\text{hom}} = 0.012$ cm^{-1} this would require more than ten transfer steps in order for such a broadening to become observable.

In general the two R lines are well correlated in crystalline Cr^{3+} materials.[21] Preliminary nonresonant FLN experiments on [Rh(bpy)$_3$][NaCr(ox)$_3$]ClO$_4$ with the excitation tuned to the R_2 line at 1.8 K also result in multiline spectra, showing the two states to be well correlated in this system, too.

A. A quantitative model

The resonant energy-transfer process within the R_1 line can be described by the following set of differential equations:

$$\frac{dN_{ei}}{dt} = -N_{ei}[k_r + k_{et}(N_{ai-1} + N_{bi+1})] + k_{et}(N_{ei+1}N_{ai}$$

$$+ N_{ei-1}N_{bi}) + \delta_{0i}k_a^{\text{ex}}N_{ai} + \delta_{1i}k_b^{\text{ex}}N_{bi}. \qquad (1)$$

In Eq. (1) $k_r = k_a + k_b$ is the sum of the individual radiative rate constants of the two transitions $e \rightarrow g_a$ and $e \rightarrow g_b$. k_a^{ex} and k_b^{ex} are the excitation rate constants for the two transitions, for which the relation $k_a^{\text{ex}}/k_b^{\text{ex}} = k_a/k_b$ holds. N_{ai}, N_{bi}, and N_{ei} are the populations of the three levels in set i, k_{et} is the bimolecular energy transfer rate constant, and δ is the delta function.

As no evident transient hole-burning was observed at the low laser powers used, it is assumed that $N_{ei} \ll N_{ai}, N_{bi}$. Therefore $N_{ai} + N_{bi} \approx N_{0i}$ holds, where N_{0i} is the total number of complexes in subset i. Furthermore, assuming a com-

paratively fast spin-lattice relaxation time for the ground state, N_{ai} and N_{bi} are given by a Boltzmann distribution

$$N_{ai} = N_{0i}/[1 + \exp(-D/k_B T)]$$

and

$$N_{bi} = N_{0i}\exp(-D/k_B T)/[1 + \exp(-D/k_B T)]. \qquad (2)$$

The values for N_{0i}, in turn, are determined by the Gaussian distribution

$$N_{0i} = N_0 \exp\left\{-\frac{4\ln 2(\tilde{\nu}_{\text{ex}} + iD - \tilde{\nu}_a)^2}{\Gamma_{\text{inh}}^2}\right\}, \qquad (3)$$

where N_0 is the density of complexes within a homogeneous linewidth at the center of the distribution. $\tilde{\nu}_a$ is the energy of the maximum of the absorption of the transition $g_a \rightarrow e$ and $\tilde{\nu}_{\text{ex}}$ is the excitation energy of the laser.

For steady-state conditions, the differential equations (1) are reduced to a set of linear equations, which are straightforward to solve numerically for N_{ei}. The resulting FLN spectra can then be calculated with the intensity $P(\tilde{\nu})$ as follows:

$$P(\tilde{\nu}) \sim \sum_i N_{ei}\{k_a g(\tilde{\nu}_{ai}) + k_b g(\tilde{\nu}_{bi})\}, \qquad (4)$$

where $g(\tilde{\nu})$ is the instrumental line shape, which is assumed to be a Gaussian limited by the instrumental resolution $\Delta\tilde{\nu}_{\text{res}}$. The energies of the transitions $e \rightarrow g_{ai}, g_{bi}$ of each subset i are defined as

$$\tilde{\nu}_{ai} = \tilde{\nu}_{\text{ex}} + iD \qquad (5)$$

and

$$\tilde{\nu}_{bi} = \tilde{\nu}_{ai} - D,$$

respectively. Calculations for steady-state FLN spectra of [Rh(bpy)$_3$][NaCr(ox)$_3$]ClO$_4$ as a function of the excitation energy $\tilde{\nu}_{\text{ex}}$ were performed with the following values for the relevant experimental parameters:

$$D = 1.3 \text{ cm}^{-1}, \quad k_r = 770 \text{ s}^{-1}, \quad \Gamma_{\text{hom}} = 0.012 \text{ cm}^{-1},$$

$$k_a/k_b = k_a^{\text{ex}}/k_b^{\text{ex}} = 2.8, \quad \Gamma_{\text{inh}} = 4.4 \text{ cm}^{-1},$$

$$N_{\text{tot}} = 1.07 \times 10^{21} \text{ cm}^{-3}, \quad \tilde{\nu}_a = 14\,398.6 \text{ cm}^{-1},$$

$$T = 1.8 \text{ K}, \quad \Delta\tilde{\nu}_{\text{res}} = 0.3 \text{ cm}^{-1}.$$

N_{tot} is the total density of luminophoric units as calculated from x-ray data.[11] With the above values the density of complexes resonant within a homogeneous linewidth at the central frequency of the inhomogeneous distribution is estimated to be

$$N_0 = 2\frac{\Gamma_{\text{hom}}}{\Gamma_{\text{inh}}}N_{\text{tot}} = 6 \times 10^{18} \text{ cm}^{-3}. \qquad (6)$$

The pseudo first-order rate constant k'_{et} is then defined as $k'_{et} = k_{et}N_0$. Thus the energy-transfer rate constant k'_{et} is the

only free parameter. For the actual calculation it is preferable to use the experimentally determined inhomogeneous distribution from the excitation spectrum of Fig. 2 rather than a Gaussian distribution according to Eq. (3) with Γ_{inh} equal to the above value. In particular the deviations from a simple Gaussian on the low-energy side of the distribution are not negligible for a quantitative evaluation of the data.

Figure 3 shows the calculated FLN spectra with k'_{et} fixed at 10^4 s^{-1}, and for different values of $\tilde{\nu}_{ex}$. The energy difference between excitation energy and the maximum of the absorption $\tilde{\nu}_{ex} - \tilde{\nu}_a$ is indicated in the figure. The resulting relative intensities in the calculated steady-state spectra are in excellent agreement with the experiment.

For simulations of the decay curves it is necessary to integrate the set of differential equations explicitly. This was done using numerical techniques with the same set of parameters as above. In Fig. 6(b) the calculated decay curves for the excitation energy $\tilde{\nu}_{ex} = 14\ 399.7$ cm^{-1} and $k'_{et} = 10^4$ s^{-1}, as determined from the steady-state spectra, are shown. The calculated curves show good agreement with the experimental curves. The deviations shortly after the pulse are due to the experimental difficulty in fully separating the individual peaks (see above).

B. The mechanism for the resonant process

Radiative energy-transfer processes are not very probable, given that thin layers of polycrystalline material with a crystalline size of less than 10 μm were used, and they can be definitely excluded on the basis of the build-up of the luminescence observed for the low-energy members of the series of peaks. Magnetic exchange interactions are negligible in $[Rh(bpy)_3][NaCr(ox)_3]ClO_4$ because the $[Cr(ox)_3]^{3-}$ units are separated by at least 9.7 Å ,[11] and with a bridging sequence Cr-ox-Na-ox-Cr no superexchange pathway is possible. Furthermore, the resonant process, in general, does not occur between nearest neighbors, because the concentration of resonant species is much lower than the total concentration of chromophores.

The most probable mechanism for such a comparatively long-range resonant process is a dipole-dipole mechanism, the probability of which is given by[22]

$$w_{DA} = \text{const} \frac{Q_A \Omega_{DA}}{\tau^r_D R^6_{DA} \tilde{\nu}^4_{DA}} = \frac{1}{\tau^r_D} \left(\frac{R_c}{R_{DA}} \right)^6, \quad (7)$$

where Q_A is the integrated absorption cross section of the acceptor, Ω_{DA} is the spectral overlap integral of the normalized absorption and emission of the acceptor and the donor, respectively, τ^r_D is the radiative lifetime of the donor, R_{DA} is the donor-acceptor separation, and $\tilde{\nu}_{DA}$ is the transferred energy. For Q_A, Ω_{DA}, and R_{DA} in units of cm, τ^r_D in seconds, and $\tilde{\nu}_{DA}$ in cm^{-1}, const takes on a value of 2.7×10^{-5}.

The critical distance R_c for which the rate of resonant energy transfer via a dipole-dipole mechanism is equal to the radiative lifetime of the donor can thus be estimated from experimentally accessible quantities. The values of τ^r_D and $\tilde{\nu}_{DA}$ are given above. The integrated absorption cross section can be calculated according to[23]

$$Q_A = 3.81 \times 10^{-21} \int \varepsilon(\tilde{\nu}) d\tilde{\nu} \approx 6 \times 10^{-19} \text{ cm}, \quad (8)$$

taking values of ε_{max} and the full width at half maximum of the R_1 line as ~ 20 lMol cm and ~ 7 cm^{-1}, respectively, from the absorption spectrum at 20 K given in Ref. 11. The spectral overlap integral for resonant energy transfer between the electronic origins of identical donors and acceptors is simply given by the integral of the square of the normalized homogeneous line shape function, which for a Lorentzian $g(\tilde{\nu})$ gives

$$\Omega_{DA} = \int g(\tilde{\nu})^2 d\tilde{\nu} = \frac{1}{\pi \Gamma_{hom}} \approx 27 \text{ cm}, \quad (9)$$

using the above value for Γ_{hom}. This results in a value for R_c of ~ 47 Å . With the above value for N_0, an excited complex at the center of the inhomogeneous distribution will have at least ~ 2 complexes in the same set to which resonant energy transfer is possible within this radius, plus an approximately equal number in the neighboring sets. Thus a resonant dipole-dipole mechanism can account for the experimentally observed energy-transfer rates.

V. CONCLUSIONS

We conclude that in $[Rh(bpy)_3][NaCr(ox)_3]ClO_4$ energy transfer within the R_1 line of the ^2E state is predominantly a *resonant* process at 1.8 K, whereas a phonon-assisted process takes over at temperatures above 3.5 K. The time-resolved FLN experiments clearly differentiate between the two. With all the other relevant parameters determined independently, the observed multiline FLN spectra are adequately described using a single rate constant for the energy-transfer process itself.

There are two reasons for the faster *resonant* process in this system as compared to ruby. (a) Because this is not a doped system and because of the more than one order of magnitude larger homogeneous linewidth [0.012 cm^{-1} versus <0.001 cm^{-1} (Ref. 24)], the concentration of centers which are resonant with each other is more than one order of magnitude larger than in ruby doped with 0.9% Cr^{3+}. (b) With a radiative lifetime of 1.3 ms, as opposed to 3.5 ms for ruby, the oscillator strength of the $^4A_2 \rightarrow {}^2E$ transition in the $[Cr(ox)_3]^{3-}$ chromophore is larger by a factor of 2.5. The somewhat smaller inhomogeneous linewidth in ruby (1.8 cm^{-1} at 0.9% doping level[4]) counteracts the above to some extent, but cannot override their combined effect. The specific nuclear structure of the three-dimensional oxalate network inhibits the formation of exchange coupled pairs, which in ruby act as shallow traps and prevent experiments at higher Cr^{3+} concentrations.

ACKNOWLEDGMENTS

[*]Current address: Département de chimie physique, Université de Genéve, 30 Quai Ernest-Ausermet, CH-1211 Geneva 4, Switerland.

[1]G. F. Imbusch and W. M. Yen, in *Laser, Spectroscopy and New Ideas*, edited by W. M. Yen and M. D. Levenson, Springer Series, in Optical Sciences, Vol. 54 (Springer-Verlag, Berlin, 1987), p. 248.

[2]G. Blasse, in *Energy Transfer Processes in Condensed Matter*, Vol. 114 of Nato Advanced Study Institute Series B, edited by B. DiBartolo (Plenum, New York, 1984), p. 251.

[3]P. M. Selzer, D. S. Hamilton, and W. M. Yen, Phys. Rev. Lett. **38**, 858 (1977).

[4]P. M. Selzer, D. L. Huber, B. B. Barnett, and W. M. Yen, Phys. Rev. B **17**, 4979 (1978).

[5]T. Holstein, S. K. Lyo, and R. Orbach, Phys. Rev. Lett. **36**, 891 (1976).

[6]S. Chu, H. M. Gibbs, S. L. McCall, and A. Passner, Phys. Rev. Lett. **45**, 1715 (1980).

[7]P. E. Jessop and A. Szabo, Phys. Rev. Lett. **45**, 1712 (1980).

[8]E. Duval and A. Monteil, in *Energy Transfer Processes in Condensed Matter* (Ref. 2), p. 643.

[9]A. Wasiela, Y. Merle d'Aubigne, and D. Bock, J. Lumin. **36**, 11 (1986); **36**, 24 (1986).

[10]A. Hauser, H. Riesen, R. Pellaux, and S. Decurtins, Chem. Phys. Lett. (to be published).

[11]S. Decurtins, H. W. Schmalle, R. Pellaux, P. Schneuwly, and A. Hauser, Inorg. Chem. **35**, 1451 (1996).

[12]S. Sugano, Y. Tanabe, and H. Kamimura, *Multiplets of Transition Metal Ions*, Pure and Applied Physics Vol. 33 (Academic, New York, 1970).

[13]T. Schönherr, J. Spanier, and H. H. Schmidtke, J. Phys. Chem. **93**, 5959 (1989).

[14]S. Decurtins, H. W. Schmalle, P. Schneuwly, J. Ensling, and P. Gütlich, J. Am. Chem. Soc. **116**, 9521 (1994).

[15]H. Riesen, J. Lumin. **54**, 71 (1992).

[16]Advanced Continuous Simulation Language (ACSL), Reference Manual, Mitchell and Gauthier Associates, Concord, Mass. 01742.

[17]S. Decurtins, R. Pellaux, A. Hauser, and M. E. von Arx, in *Magnetism-a Molecular Function*, edited by O. Kahn (Kluwer, Dortrecht, in press).

[18]A. Szabo, Phys. Rev. Lett. **27**, 323 (1971).

[19]P. W. Anderson, Phys. Rev. **109**, 1492 (1958).

[20]P. W. Anderson, Comments Solid State Phys. **2**, 193 (1970).

[21]H. Riesen and E. Krausz, Comments Inorg. Chem. **14**, 323 (1993).

[22]G. Blasse, Philips Res. Rep. **24**, 131 (1969).

[23]J. B. Birks, *Photophysics of Aromatic Molecules* (Wiley, New York, 1970), p. 44.

[24]P. E. Jessop, T. Muramato, and A. Szabo, Phys. Rev. B **21**, 926 (1980).